

Single-crystal Raman spectroscopy of natural schafarzikite FeSb_2O_4 from Pernek, Slovak Republic

SILMARILLY BAHFENNE, LLEW RINTOUL, AND RAY L. FROST*

Chemistry Discipline, Faculty of Science and Technology, Queensland University of Technology, GPO Box 2434, Brisbane, Queensland 4001, Australia

ABSTRACT

We present the first single-crystal Raman spectra of the mineral schafarzikite FeSb_2O_4 from the Pernek locality of the Slovak Republic. In addition, Raman spectra of the natural mineral apuanite $\text{Fe}^{2+}\text{Fe}_4^{3+}\text{Sb}_4\text{O}_{12}\text{S}$, originating from the Apuan Alps in Italy, as well as spectra of synthetic ZnSb_2O_4 and the arsenite mineral trippkeite (CuAs_2O_4) are presented for the first time. The spectra of the antimonite minerals are characterized by a strong band in the region 660–680 cm^{-1} with shoulders on either side, and a band of medium intensity near 300 cm^{-1} . The spectrum of the arsenite mineral is characterized by a medium band near 780 cm^{-1} with a shoulder on the high wavenumber side and a strong band at 370 cm^{-1} . Mode assignments are proposed based on the spectral comparison between the compounds, symmetry modes of the bands and prior literature. The single-crystal spectra of schafarzikite showed good mode separation, allowing bands to be assigned to the symmetry species of A_{1g} , B_{1g} , B_{2g} , or E_g .

Keywords: Schafarzikite, trippkeite, apuanite, single-crystal Raman spectroscopy, antimonite

INTRODUCTION

As part of a larger study of arsenite and antimonite minerals (Bahfenne and Frost 2010a, 2010b, 2010c; Frost and Bahfenne 2010a, 2010b; Bahfenne et al. 2010), we report the single-crystal Raman spectrum of natural schafarzikite FeSb_2O_4 and the non-oriented Raman spectra of its Zn analog and the related minerals, apuanite and trippkeite. Schafarzikite is a meta-antimonite mineral containing polymeric SbO_3 pyramids and crystallizes in the tetragonal space group $P4_2/mbc$ (D_{4h}^{13}), $a = 8.59$ and $c = 5.92$ Å, $Z = 4$ (Zemann 1951a; Fischer and Pertlik 1975; Sejkora et al. 2007). Schafarzikite is isostructural to trippkeite CuAs_2O_4 , which was the first mineral characterized to possess AsO_3 chain-like polymers (Zemann 1951b), others being the synthetic compound NaAsO_2 (Menary 1958; Lee and Harrison 2004) and the mineral leiteite ZnAs_2O_4 (Bahfenne et al. 2010; Ghose et al. 1987). The crystal studied is dark brown with a metallic luster, and originated from Pernek, Malé Karpaty Mountains, Slovak Republic. It is also known to occur at Buca della Vena, Apuan Alps, Italy, commonly associated with and closely related to other antimonites such as versiliaite $\text{Fe}_3^{2+}\text{Fe}_4^{3+}\text{Sb}_6\text{O}_{16}\text{S}$ and apuanite $\text{Fe}^{2+}\text{Fe}_4^{3+}\text{Sb}_4\text{O}_{12}\text{S}$ (Mellini et al. 1979; Mellini and Merlino 1979).

A comparison of chemical formulas may tempt one to conclude that leiteite is isostructural to schafarzikite and trippkeite, when in fact this is not the case. In trippkeite and schafarzikite, the cation is found in octahedral geometry surrounded with six O atoms, whereas in leiteite the cation is found in an open tetrahedral geometry. Leiteite also shows a different arrangement of the O atoms around the As; the bridging O connect only As together, whereas for schafarzikite-like structures the so-called bridging O atom is bound to the cation in addition to bridging the two As atoms. A more detailed discussion can be found in the description of crystal structure section below.

To our knowledge, a single-crystal Raman study has not been attempted previously, although non-oriented Raman and IR spectra of schafarzikite from the Pernek locality has been published (Sejkora et al. 2007). To aid assignments, comparisons were made with the spectra of synthetic antimonites of manganese and nickel, found in literature (Chater et al. 1986). Additionally ZnSb_2O_4 and trippkeite CuAs_2O_4 were synthesized and their Raman spectra recorded. Raman experiments were also performed on crystals of apuanite. The single-crystal spectra enabled the assignment of modes to their symmetry.

DESCRIPTION OF CRYSTAL STRUCTURE

Schafarzikite is tetragonal with space group $P4_2/mbc$ (D_{4h}^{13}) and four formula units per unit cell. The crystal cell dimensions are $a = 8.59$ and $c = 5.91$ Å (Zemann 1951a; Fischer and Pertlik 1975). The structural building blocks of schafarzikite consist of the octahedrally coordinated Fe and the Sb trigonal pyramidal geometry. Columns of edge-sharing FeO_6 octahedra run parallel to [001], on either side of, which are chains of corner sharing $[\text{SbO}_3]^{3-}$ groups. The symmetry of the SbO_3 pyramids is reduced to C_s from the ideal trigonal pyramid (C_{3v}) symmetry. Open channels parallel to [001] are also found within the framework (Mellini and Merlino 1979). There are two kinds of O atoms, O1 and O2. Each Sb is connected to two O1 and one O2 and each Fe is connected to four O2 and two O1. The above arrangement of O atoms is observed in several compounds with similar building blocks, e.g., natural minerals trippkeite (CuAs_2O_4) and apuanite ($\text{Fe}^{2+}\text{Fe}_4^{3+}\text{Sb}_4\text{O}_{12}\text{S}$), and synthetic ZnSb_2O_4 , NiSb_2O_4 , and MnSb_2O_4 . However it is different from the one found in other known antimonite compounds. Röhr showed that in synthetic antimonites of formulas ASbO_2 and $\text{A}_4\text{Sb}_2\text{O}_5$, where A = K, Rb, Cs, and some O atoms could be definitively characterized as bridging (those that only connect two Sb atoms together) and others as terminal (those that link the Sb atom to the other metal atom) (Hirschle and Röhr 2000). In schafarzikite, O1 can be

* E-mail: r.frost@qut.edu.au

considered to be the bridging O, even though it also connects Sb to Fe, because it connects two Sb atoms together, whereas O2 does not. Positional parameters indicate that Fe occupy $4d$ or D_2' , Sb, and O2 on $8h$ or C_8' , and O1 on $8g$ or C_2' . The Sb-O1 and Sb-O2 bond lengths are 1.987 and 1.917 Å, respectively. As in the case of the antimonites mentioned above, the distance from Sb to a terminal O atom is shorter than that to a bridging O atom.

The structure of apuanite can be derived from that of schafarzikite by substitution of every third Sb^{3+} in the chain with Fe^{3+} , and insertion of S^{-} in the open channels between the two Fe^{3+} atoms facing each other in adjacent chains. Furthermore two thirds of Fe^{2+} in the FeO_6 columns in schafarzikite are oxidized to Fe^{3+} in apuanite (Mellini and Merlino 1979). Unlike schafarzikite where there are two types of O atoms connected to Sb apuanite has three types of O atoms due to the substitution of every third Sb with Fe^{3+} . The terminal Sb-O bond is 1.975 Å, and the two bridging bonds, Sb-O-Sb and Sb-O-Fe, are 2.006 and 1.964 Å, respectively.

The structure of trippkeite was first solved by Zemanz (1951b) and later refined by Pertlik (1975). The cell dimensions of trippkeite are $a = 8.59$ and $c = 5.57$ Å (Pertlik 1975), and As-O1 and As-O2 bond lengths are 1.814 and 1.765 Å, respectively. Cu and As replace Fe and Sb, respectively, in the schafarzikite structure.

EXPERIMENTAL METHODS

Crystals of schafarzikite and apuanite were supplied by the National Museum in the Czech Republic and the Mineralogical Research Museum, respectively. Schafarzikite originated from the Pernek-Križnica locality in the Malé Karpaty Mountains in the Slovak Republic, whereas the apuanite specimen is from Buca della Vena in the Apuan Alps, Italy.

$ZnSb_2O_4$ was prepared by adjusting the procedures to prepare $UO_2Sb_2O_4$ given by Sykora et al. (2004). A mixture of 4 g of Sb_2O_3 and 1.12 g of ZnO (0.01375 mol) reacted hydrothermally in 20 mL H_2O at 180 °C for 89 h and cooled at a rate of 10 °C/h. The product appeared as white crystals dispersed in white powder, which is possibly undissolved Sb_2O_3 . The two were separated manually after filtering from mother liquor, washing several times with deionized water, and drying in an oven at 150 °C overnight. Trippkeite was synthesized following the procedures given by Pertlik (1977). 2.2 g of As_2O_3 and 0.88 g of CuO reacted hydrothermally in 80 mL 1 M CH_3COOH at 210 °C for approximately 2 days and cooled naturally. The product appeared as dark green needles covered with red metallic wires. During filtration the product was washed several times with deionized water, and then dried at 110 °C overnight.

The crystalline materials were characterized by X-ray powder diffraction (XRD). The XRD analyses were carried out on a Philips wide-angle PW 1050/25 vertical goniometer (Bragg Brentano geometry) applying $CuK\alpha$ radiation ($\lambda = 1.54$ Å, 40 kV, 40 mA). The samples were measured in step scan mode with steps of 0.02 ° 2θ and a scan speed of 1.00 ° per min from 2 to 75 ° 2θ .

Scanning electron microscope (SEM) photos were obtained on a FEI QUANTA 200 environmental scanning electron microscope operating at high vacuum and 15 kV. This system is equipped with an energy-dispersive X-ray spectrometer with a thin Be window capable of analyzing all elements of the periodic table down to carbon. For the analysis, a counting time of 100 s was applied.

For the Raman spectroscopy, we used a Renishaw 1000 Raman microscope system, which also includes a monochromator, a Rayleigh filter system, and a CCD detector coupled to an Olympus BHSM microscope equipped with 10× and 50× objectives. The Raman spectra were excited by a Spectra-Physics model 127 He-Ne laser producing plane polarized light at 633 nm and collected at a resolution of better than 4 cm^{-1} and a precision of ± 1 cm^{-1} in the range between 120 and 4000 cm^{-1} . Repeated acquisitions on the crystals using the highest magnification (50×) were accumulated to improve the signal-to-noise ratio in the spectra. The instrument was calibrated prior to use using the 520.5 cm^{-1} line of a silicon wafer. In the normal course of spectral accumulation, 20 scans were accumulated at 20 s time intervals.

A crystal of schafarzikite was selected and placed on the corner of a perfect cube, aligned parallel to the sides of the cube using a very fine needle. In the plane

of the schafarzikite flake, the long axis corresponded to the c axis, the b axis was at right angles in the same plane as the long axis, and the a axis is normal to the b - c plane. Thus, the rotation of the cube through 90° around the X , Y , and Z axes of the laboratory frame allowed an interrogation of the three crystallographic axes. The Raman spectra of the oriented single crystals are reported in accordance with the Porto notation (Damen et al. 1966): the propagation directions of the incident and scattered light and their polarizations are described in terms of the crystallographic axes a , b , and c . The notation may, for example read CABC. Here the first C is the direction of the incident light, A is the direction of the polarization of the electric vector of the incident light, B is the orientation of the analyzer, and the second C is the direction of the propagation of the scattered light.

Spectral manipulation such as baseline correction/adjustment was performed using the GRAMS software package (Galactic Industries Corporation, New Hampshire, U.S.A.) and component analysis was undertaken using the Jandel "Peakfit" software package (version 1) that enabled the type of fitting function to be selected and allows specific parameters to be fixed or varied accordingly. Band fitting was done using a Lorentzian-Gaussian cross-product function with the minimum number of component bands used for the fitting process. The Lorentzian-Gaussian ratio was maintained at values greater than 0.7 and fitting was undertaken until reproducible results were obtained with squared correlations of R^2 greater than 0.995.

RESULTS

X-ray diffraction

The product of $ZnSb_2O_4$ synthesis was subjected to XRD analysis (Fig. 1a). The major phase of the white powder was Sb_2O_3 , with minor phases of ZnO and $ZnSb_2O_4$, while that of the crystal was $ZnSb_2O_4$. Although the crystals were separated as well as possible from the powder, they were still covered in the powder causing the XRD pattern of the crystal to show lines corresponding to Sb_2O_3 and ZnO (both minor). Figure 1b shows XRD analysis of the product of trippkeite synthesis. Rietveld refinement showed the product to consist of approximately 65% trippkeite, 20% CuO and 14% Cu_2O and negligible amounts of copper arsenates olivenite and cornubite.

Scanning electron microscopy

SEM images (Figs. 2a–2b) of natural schafarzikite and synthetic $ZnSb_2O_4$ show the columnar nature of the compounds. Crystals with flat surfaces and a size greater than 100 μm are suitable for single-crystal Raman spectroscopy experiments. The SEM image (Fig. 2c) of synthetic trippkeite shows the majority of crystals to be 10 μm or less in size, with some being about 20 μm . While the size and the needle morphology of the crystals was well suited to single-crystal Raman experiments, the aggregation and small size of the crystals made it difficult to isolate a single crystal.

Factor group analysis

The unit cell of schafarzikite is the primitive unit cell and it contains four formula units. Thus a primitive unit cell contains 28 atoms. The number of allowable modes is 81 consisting of $5A_{1g} + 7A_{2g}$ (IA) + $7B_{1g} + 5B_{2g} + 3A_{1u}$ (IA) + $5A_{2u} + 5B_{1u}$ (IA) + $3B_{2u}$ (IA) + $9E_g + 13E_u$ (IA = inactive). The form of the polarizability tensor for D_{4h} crystals dictates that A_{1g} modes are observed in the AA, BB, and CC orientations, B_{1g} in AA and BB, B_{2g} in AB, and E_g in AC and BC. Schafarzikite is uniaxially positive ($\omega > 1.74$, $\epsilon = n.d.$), with the only optic axis parallel to the c axis. The difference in velocities between the ordinary and extraordinary rays is 0 when light travels along the optic axis and maximum 90° away. In a tetragonal crystal such as schafarzikite, $\alpha = \beta = \gamma = 90^\circ$ so light traveling along any axes other than c will

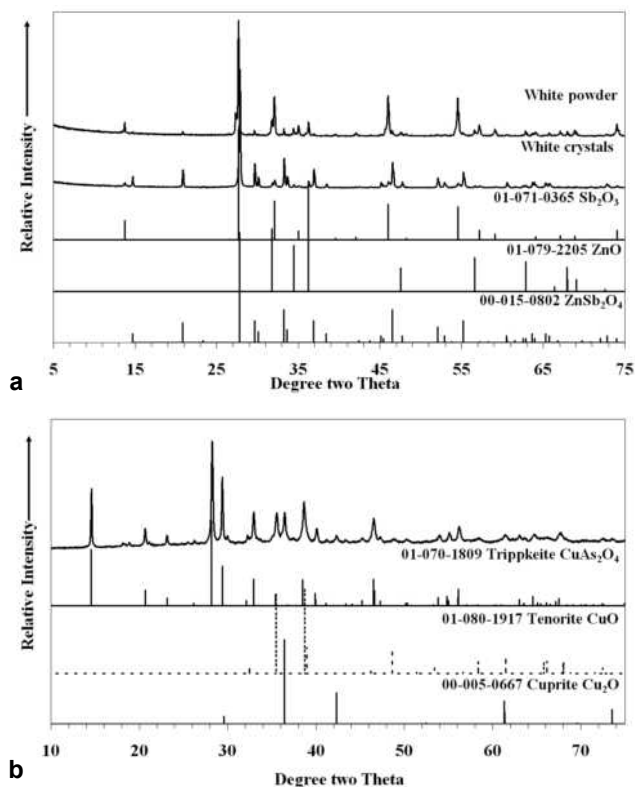


FIGURE 1. XRD patterns of the products formed in (a) ZnSb_2O_4 and (b) CuAs_2O_4 syntheses.

experience birefringence, although weakly in this case since no scrambling of incident radiation was observed in spectra taken from **a** or **b** faces.

Discussion of the Raman spectroscopy

Schafarzikite. The Raman spectrum of non-oriented natural schafarzikite, as shown in Figure 3, is characterized by a very intense band at 668 cm^{-1} and medium bands at 295 , 159 , and 107 cm^{-1} . These peak positions compare favorably to those found previously (Sejkora et al. 2007), but peak-fitting reveals several bands that were hitherto unreported, such as the small band at 709 cm^{-1} underlying the most intense band and weak bands at 479 and 186 cm^{-1} . Extra bands are also detected in the lower wavenumber range at 132 , 119 , and 107 cm^{-1} . Also previously unreported are two broad bands at 1388 and 1031 cm^{-1} (not shown) that are very weak relative to other bands. Although the band at 709 cm^{-1} is weak relative to the overlying band, its existence is unambiguous. Without the band at 709 cm^{-1} , there would be unaccounted intensity on the high wavenumber side of the strong band. A summary of peak positions found in the current work and previously are tabulated in Table 1.

The oriented single-crystal spectra of schafarzikite are displayed in Figures 4a–4b. Good separation between different symmetry species is observed. The band at 668 cm^{-1} is very strong in the CAAC and CBBC spectra, and its intensity does not diminish significantly in the ACCA spectrum and thus is assigned as A_{1g} , and the shoulder at 709 cm^{-1} is assigned to the B_{1g} symmetry mode. The shoulder on the low wavenumber side, at 617 cm^{-1} is strongest in the CABC spectrum and is assigned to

TABLE 1. Peak-fitted results of Raman spectra of schafarzikite and ZnSb_2O_4 of the current study, and peak positions of Raman spectra of schafarzikite, MnSb_2O_4 , and NiSb_2O_4 of prior literature

Schafarzikite		Trippkeite		Assignment
Band Position (cm^{-1})	Symmetry	Band Position (cm^{-1})	Symmetry	
709	B_{1g}	810	?	Sb(As)-O terminal
668	A_{1g}	780	A_{1g}	
617	B_{2g}			Sb(As)-O bridging
558	E_g			
526	B_{1g}	657	B_{1g}	Sb(As)-O deformation
539	B_{1g}			
465	A_{1g}	496	A_{1g}	Sb(As)-O deformation
403	E_g			
353	B_{1g}	421	B_{1g}	Sb(As)-O deformation
345	B_{2g}			
295	A_{1g}	371	A_{1g}	Lattice modes
249	B_{2g}			
219	B_{1g}			Lattice modes
208	B_{2g}			
186	?			Lattice modes
159	A_{1g}			
132	E_g			Lattice modes
119	B_{2g}			
107	B_{1g}			Lattice modes

B_{2g} symmetry. The very weak bands at 558 and 403 cm^{-1} apparent in the peak-fitted spectrum cannot clearly be seen in Figure 4 but on magnification it appears to be the most defined in ABCA and thus E_g is a possible symmetry for these modes. The bands at 526 and 465 cm^{-1} are assigned to B_{1g} and A_{1g} , respectively, the weak underlying band at 478 cm^{-1} is assigned to the B_{1g} . The band around 350 cm^{-1} appears to have only one component in the peakfitted spectrum, but the oriented spectra clearly show two closely spaced bands at 353 (B_{1g}) and 345 cm^{-1} (B_{2g}). A band at 295 cm^{-1} , which is strongest in CAAC and CBBC spectra is assigned to be of A_{1g} symmetry since its intensity is still significant in the ACCA spectrum.

ASb_2O_4 (A = Zn, Ni, Mn). Synthetic antimonites isostructural to schafarzikite include those of zinc, nickel and manganese. The non-oriented Raman spectrum of ZnSb_2O_4 is shown in Figure 5a. Raman spectra of NiSb_2O_4 and MnSb_2O_4 may be found in Figure 2 of Chater et al. (1986). The spectrum in the region 250 – 900 cm^{-1} is very similar in all the above ASb_2O_4 compounds and it may be concluded that this region corresponds to Sb-O vibrations with minimal contribution from the cations. The peak position and intensities of these compounds are also summarized in Table 1. Spectra of NiSb_2O_4 and MnSb_2O_4 were not peak-fitted so the band list is not necessarily complete, for instance the bands at the highest wavenumber (685 and 670 cm^{-1} , respectively) were not reported to have shoulders but the fact that they are broad makes the existence of shoulders possible as is found in ZnSb_2O_4 and schafarzikite.

Single-crystal studies of NiSb_2O_4 and MnSb_2O_4 were not attempted due to insufficient crystal size. The synthesis of ZnSb_2O_4 , however, did give suitable crystals and thus we attempted a single-crystal study to compare its symmetry assignments to those of schafarzikite. It was found that the major band at around 670 cm^{-1} and both its shoulders have the same symmetry as their corresponding bands in schafarzikite, (681 and 675 cm^{-1} : A_{1g} , 634 cm^{-1} : B_{2g} in ZnSb_2O_4). Weak E_g bands were also observed in the spectra of both compounds at 550 – 570 and 400 – 420 cm^{-1} . The A_{1g} symmetry of the band near 295 cm^{-1} is also replicated in ZnSb_2O_4 .

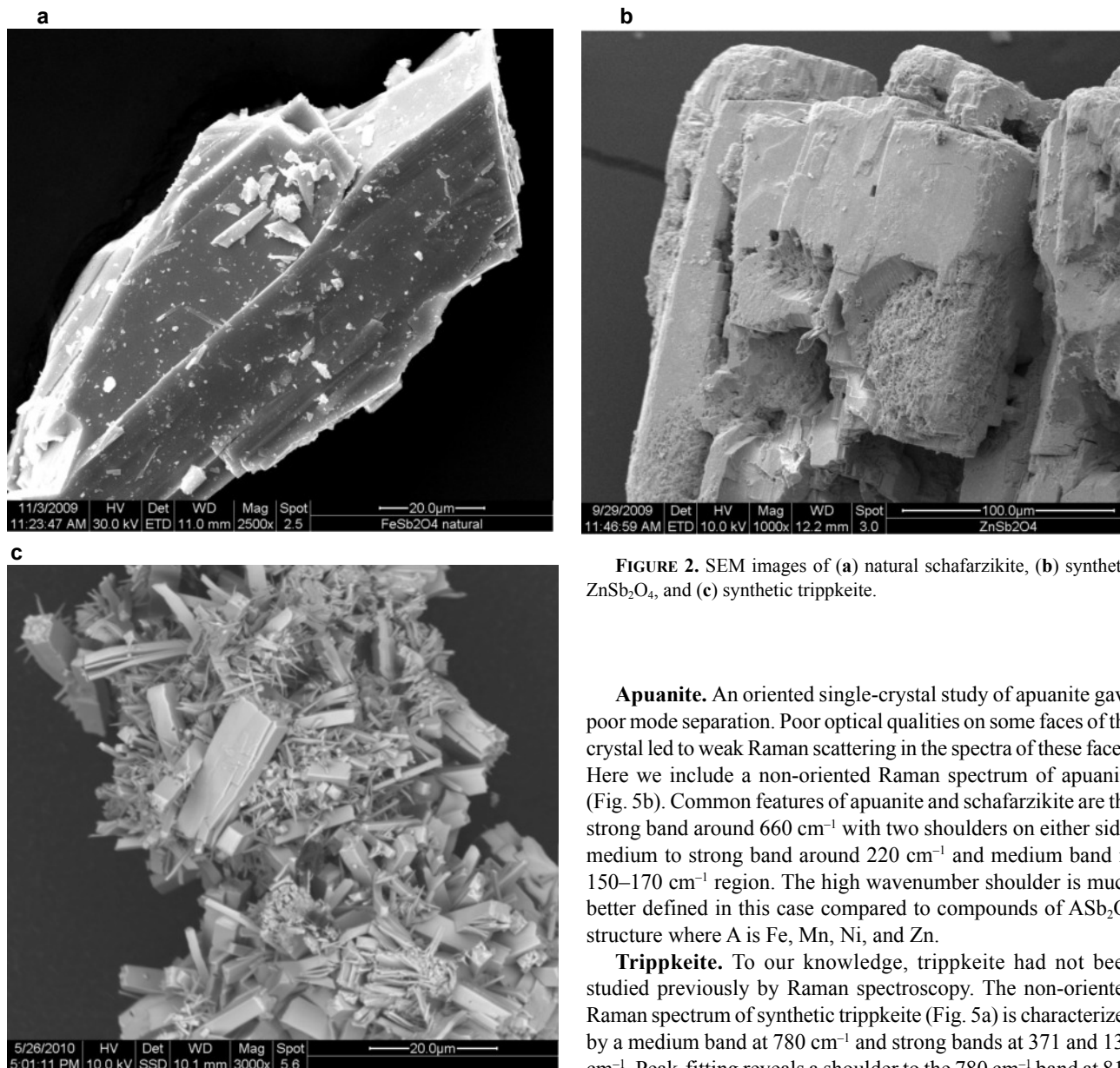


FIGURE 2. SEM images of (a) natural schafarzikite, (b) synthetic ZnSb_2O_4 , and (c) synthetic trippkeite.

Apuanite. An oriented single-crystal study of apuanite gave poor mode separation. Poor optical qualities on some faces of the crystal led to weak Raman scattering in the spectra of these faces. Here we include a non-oriented Raman spectrum of apuanite (Fig. 5b). Common features of apuanite and schafarzikite are the strong band around 660 cm^{-1} with two shoulders on either side, medium to strong band around 220 cm^{-1} and medium band in $150\text{--}170\text{ cm}^{-1}$ region. The high wavenumber shoulder is much better defined in this case compared to compounds of ASb_2O_4 structure where A is Fe, Mn, Ni, and Zn.

Trippkeite. To our knowledge, trippkeite had not been studied previously by Raman spectroscopy. The non-oriented Raman spectrum of synthetic trippkeite (Fig. 5a) is characterized by a medium band at 780 cm^{-1} and strong bands at 371 and 134 cm^{-1} . Peak-fitting reveals a shoulder to the 780 cm^{-1} band at 810 cm^{-1} , and a second component to both strong bands at 371 and 134 cm^{-1} . The general appearance of the spectrum is similar to the spectrum of schafarzikite except that the bands are shifted to higher wavenumbers, as expected owing to the lighter As atom. Thus, the relevant AsO_3 peaks lie above $\sim 300\text{ cm}^{-1}$. The fact that the crystals are small and aggregated made the isolation and manipulation of a single crystal difficult and thus oriented Raman experiments were incomplete. However, we were able to assign tentatively the A_{1g} and B_{1g} bands by examining the CC and AA/BB spectra, which were readily obtained due to the position of the crystal. The CC spectrum was obtained by aligning the plane of the laser parallel to the longest axis of the crystal, and the AA/BB spectrum by aligning the laser parallel to the axis at right angle to the longest axis. The medium band at 780 cm^{-1} is of A_{1g} symmetry, as well as the weak band at 496 cm^{-1} and the strong band at 371 cm^{-1} . The schafarzikite counterparts of the above bands are 668 , 465 , and 295 cm^{-1} . Those belonging to B_{1g} symmetry include the bands at 657 , 539 , and 421 cm^{-1} (526 ,

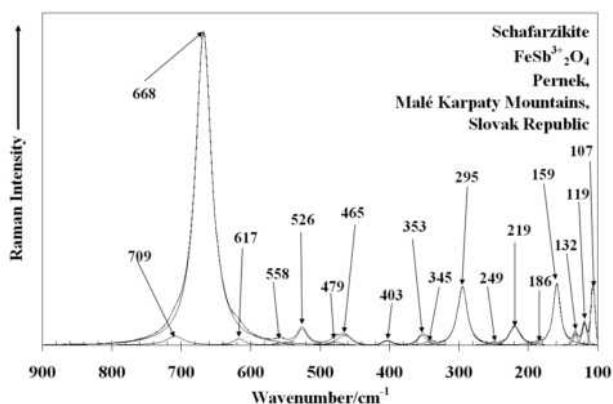


FIGURE 3. Peak-fitted Raman spectrum of schafarzikite in the $900\text{--}100\text{ cm}^{-1}$ region.

479, and 353 cm^{-1} in schafarzikite). It is observed that the order of the band symmetries in trippkeite match that of schafarzikite. The partial symmetry assignment of the bands in the trippkeite spectrum is presented in Table 2.

DISCUSSION

Out of the 35 allowable Raman modes of schafarzikite, 22 modes were observed consisting of $4A_{1g} + 5B_{1g} + 5B_{2g} + 4E_g$. Two types of Sb-O stretches can be expected in schafarzikite-like structures corresponding to terminal and bridging O atoms. The symmetry of SbO_3 is reduced from the ideal trigonal pyramid (C_{3v}) symmetry to C_s . Under C_{3v} symmetry the two Sb-O stretching modes have A_1 symmetry and E symmetry, respectively. On a C_s site A_1 modes translate to A' and E modes split to A' and A'' . Sb and the terminal O2 atoms are located on C_s sites, so theoretically the terminal Sb-O stretch should have A' symmetry and the bridging Sb-O stretches should give two components (A' and A''). Correlating this to a D_{4h} crystal system means that each A' vibration will have A_{1g} , B_{1g} , and B_{2g} components in the Raman spectrum (A_{2g} is inactive; $2E_u$ modes are expected in the IR spectrum), and each A'' vibration will only have $2E_g$ components in the Raman spectrum (A_{1u} , B_{1u} , and B_{2u} are inactive; A_{2u} is expected in the IR spectrum). The splitting pattern is summarized in Table 3. If the factor group analysis of the ideal molecule applies to this particular case, the terminal Sb-O stretch should give rise to A_{1g} , B_{1g} , and B_{2g} components whereas the bridging Sb-O stretch should give rise to A_{1g} , B_{1g} , B_{2g} , and $2E_g$ components.

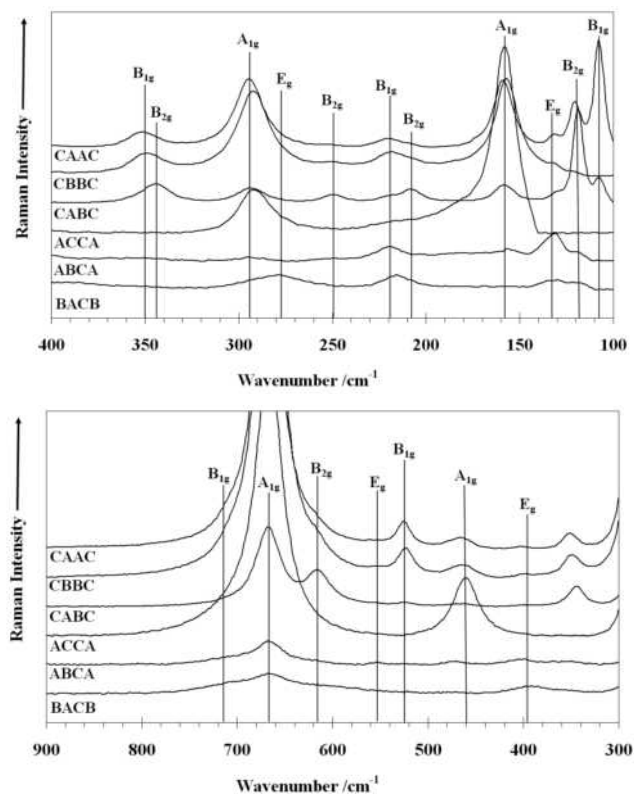


FIGURE 4. (a) Oriented single-crystal Raman spectrum of schafarzikite in the 400–100 cm^{-1} region. (b) Oriented single-crystal Raman spectrum of schafarzikite in the 900–300 cm^{-1} region.

In the Sb-O stretching region of schafarzikite the following modes are observed: 709 (B_{1g}), 668 (A_{1g}), 617 (B_{2g}), 558 (E_g), 526 (B_{1g}), and 465 cm^{-1} (A_{1g}). Symmetry considerations lead to the conclusion that one of the A_{1g} bands can be apportioned to the terminal Sb-O stretch and the other to the bridging Sb-O stretch. The same applies to the two B_{1g} bands.

A band near 700 cm^{-1} was observed by Hirschle and Röhr (2000) in Sb^{3+} compounds with the $[\text{Sb}_2\text{O}_5]^{4-}$ units possessing two terminal O and one bridging O atoms, but not observed in compounds with infinite $\text{O}_2\text{-Sb-O}_2$ chains with no terminal O atoms. By analogy, it seems likely that of the two A_{1g} and B_{1g} candidates for the terminal O stretch, the strong band at 668 cm^{-1} and the shoulder at 709 cm^{-1} are the more probable. Furthermore supporting this assignment is the observation of bands near 700 and 650 cm^{-1} by Hirschle and Röhr (2000) in Sb^{3+} compounds with the $[\text{Sb}_2\text{O}_5]^{4-}$ units (possessing two terminal O and one bridging O atoms), but not observed in compounds with infinite $\text{O}_2\text{-Sb-O}_2$ chains with no terminal O atoms.

Hirschle and Röhr (2000) also described bands near 650 and 615 cm^{-1} in both types of compounds mentioned above, thus the shoulder at 616 cm^{-1} (B_{2g}) of schafarzikite is assigned to a stretch of the bridging O unit. The relatively low wavenumber position of the E_g mode at 558 cm^{-1} , the B_{1g} mode at 526 cm^{-1} , and the A_{1g} mode at 465 cm^{-1} suggests that they are associated with bridging Sb-O.

As mentioned above theoretically there should be another B_{2g} and E_g bands, the former corresponding to stretches of the terminal Sb-O and the latter to those of bridging Sb-O. The E_g component may be too weak to be observed, or may be accidentally degenerate. The maximum number of five B_{2g} bands has been observed but there is a possibility of one or more of these being combination modes, which may justify the expectation of one more B_{2g} band corresponding to a terminal Sb-O stretch.

The observation that terminal Sb-O stretch occurs at a higher wavenumber fits in well with the shorter terminal Sb-O bond length (1.917 Å) compared to the bridging Sb-O bond length (1.987 Å). Bands around 300 cm^{-1} have been previously assigned to Sb-O deformations, thus the strong band at 295 cm^{-1} in schafarzikite is assigned likewise. The weak broad bands at 1388 and 1031 cm^{-1} are probably due to the combinations 668 + 709 cm^{-1} and 558 + 479 cm^{-1} , respectively. The partial band assignments are summarized in Table 2.

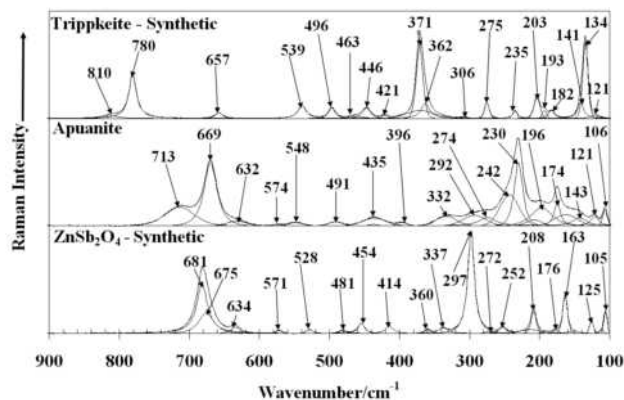


FIGURE 5. Peak-fitted Raman spectrum of ZnSb_2O_4 in the 800–100 cm^{-1} region.

TABLE 2. Peak positions, symmetry, and assignment of the oriented single-crystal spectra of schafarzikite and trippkeite

Schafarzikite			Schafarzikite [64]		Synthetic ZnSb ₂ O ₄			Synthetic NiSb ₂ O ₄ [15]		Synthetic MnSb ₂ O ₄ [15]	
Center	FWHM	%	Center	Intensity	Center	FWHM	%	Center	Intensity	Center	Intensity
1387	66.24	1.39									
1036	99.50	0.65									
709	28.96	2.31									
668	27.51	72.30	670	vs	676	21.73	36.42	685	m-s	670	vs
617	18.50	1.07	617	w-m	635	15.08	1.98	638	m	620	m
558	12.22	0.38			572	9.85	0.55	585	w	547	vw
526	16.81	2.54	524	w	528	10.72	0.76	535	w	527	m
479	17.20	0.53			482	9.75	0.57	486	w	474	m
465	24.97	1.46	467	w	454	11.65	2.55			465	m
403	16.40	0.41	405	w	414	12.59	2.25	421	w	399	w
353	15.09	1.06			360	9.58	0.71	360	m	350	m
345	14.65	0.41	348	m	338	15.61	2.36			345	m
295	16.30	3.67	295	s	298	11.28	30.05	309	vs	292	s
249	21.00	0.36	252	w-m	253	11.35	1.69	244	m	255	m
219	17.64	2.18	217	m	213	33.46	2.82			215	w
					208	8.44	4.08				
186	7.92	0.14			191	9.66	0.34	180	s	189	w-m
					177	10.35	0.71				
					164	7.89	6.56				
159	12.15	6.64	161	m-s	151	15.11	1.03	157	m	156	m
132	5.76	0.60			126	6.09	1.55	132	s	124	s
119	8.00	0.58			111	7.58	0.24	119	s	118	w
107	6.88	1.31			106	5.54	1.25			105	s

TABLE 3. Factor group analysis of the SbO₃ group in schafarzikite

Point Symmetry	Site Symmetry	Crystal Symmetry
C_{3v}	C_s	D_{4h}
$2A_1$	A'	A_{1g}
		A_{2g}
		B_{1g}
		B_{2g}
		$2E_u$
$2E$	A''	A_{1u}
		A_{2u}
		B_{1u}
		B_{2u}
		$2E_g$

The spectrum of apuanite has some common features with the spectrum of schafarzikite, including the intense band around 660 cm⁻¹ with two shoulders on either side. Using the same considerations applied to schafarzikite, bands in the region of 632–491 cm⁻¹ are assigned to vibrations of the bridging Sb-O units, and the bands at 669 and 713 cm⁻¹ are assigned to vibrations of the terminal Sb-O. A point of difference between the two spectra is the added intensity of the higher wavenumber shoulder compared to that observed in the spectra of other ASb₂O₄ compounds. As mentioned in the structural description, every third Sb is substituted by Fe causing each Sb to have three types of bonds: terminal Sb-O, bridging Sb-O-Sb, and Sb-O-Fe. The added intensity of the shoulder may be explained by the similar bond lengths of terminal Sb-O (1.975 Å) to Sb-O-Fe (1.964 Å), which causes the

vibration of the latter to occur in the same region.

The spectra assignments of trippkeite are based on the previous work by Emmerling and Röhr (2003) who conducted a Raman study on some analogous As³⁺ compounds, and a theoretical study by Tossell (1997). Emmerling and Röhr (2003) observed a band above 800 cm⁻¹ observed in compounds of the formula AAsO₂ (A = Na, K, and Rb) where the AsO₃ units are interconnected (each unit possessing one terminal O and two bridging O atoms). These bands were assigned to the vibration of terminal O. A theoretical study by Tossell (1997) presented calculated wavenumbers of the dimeric molecules As₂O(OH)₄ and [As₂O₅]⁴⁺, and assigned the terminal As-O stretches to bands in the 847–707 cm⁻¹ region, and the bridging As-O stretches to bands in the 699–496 cm⁻¹ region. Therefore, the bands at 780 and 810 cm⁻¹ in trippkeite are assigned to stretches of terminal O atoms and stretches of the bridging O atoms are assigned to bands at 657 and 496 cm⁻¹. The rest of the assignments are listed in Table 2.

The spectra of the antimonite compounds are characterized by a strong band in the region 660–680 cm⁻¹, with shoulders on either side, and a band of medium to strong intensity near 300 cm⁻¹. Spectral comparison between the antimonite compounds in this study and those in prior literature shows that the strong band near 660 cm⁻¹ corresponds to a stretch of the terminal Sb-O bond, whereas the shoulder at the lower wavenumber correspond to stretches of the bridging Sb-O bonds. Furthermore the bands in the region 616–450 cm⁻¹ are also assigned to various vibrations of the bridging Sb-O units based on their symmetry modes. Bands around 300 cm⁻¹ have also been assigned as Sb-O bends. The assignment above is confirmed by the shorter terminal Sb-O bond compared to bridging ones. The spectrum of trippkeite is dominated by a medium band at 780 cm⁻¹ with a high wavenumber shoulder and a strong band at 370 cm⁻¹ and has a similar general appearance to that of schafarzikite except that the bands are shifted to higher wavenumbers, as expected of the lighter As atom. Factor group analysis determined there should be $5A_{1g} + 7B_{1g} + 5B_{2g} + 9E_g$ in the Raman spectrum and in this

study $5A_{1g} + 4B_{1g} + 5B_{2g} + 4E_g$ were observed. Good separation between different symmetry modes is observed.

ACKNOWLEDGMENTS

The financial and infrastructure support of the Queensland University of Technology, Inorganic Materials Research Program is gratefully acknowledged. The Australian Research Council (ARC) is thanked for funding the instrumentation.

REFERENCES CITED

- Bahfenne, S. and Frost, R.L. (2010a) A review of the vibrational spectroscopic studies of arsenite, antimonite, and antimonate minerals. *Applied Spectroscopy Reviews*, 45, 101–129.
- (2010b) Raman spectroscopic study of the mineral finnemanite $Pb_5(As^{3+}O_3)_3Cl$. *Journal of Raman Spectroscopy*, 41, 329–333.
- (2010c) Raman spectroscopic study of the multi-anion mineral dixenite $CuMn_{12}Fe^{3+}(AsO_3)_5(SiO_4)_2(AsO_4)(OH)_6$. *Journal of Raman Spectroscopy*, 41, 465–468.
- Bahfenne, S., Rintoul, L., and Frost, R.L. (2010) Single-crystal Raman spectroscopy of natural leiteite ($ZnAs_2O_4$) and comparison with the synthesised mineral. *Journal of Raman Spectroscopy*, in press, DOI: 10.1002/jrs.2751.
- Chater, R., Gavarrri, J.R., and Genet, F. (1986) Composes isomorphes $MeX_2O_4E_2$: I. Etude vibrationnelle de $MnSb_2O_4$ entre 4 et 300 K: Champ de force et tenseur elastique. *Journal of Solid State Chemistry*, 63, 295–307.
- Damen, T.C., Porto, S.P.S., and Tell, B. (1966) Raman effect in zinc oxide. *Physical Review*, 142, 570–574.
- Emmerling, F. and Röhr, C. (2003) Die neuen Oxoarsenate(III) $AAsO_2$ (A = Na, K, Rb) und $Cs_3As_3O_9$. Darstellung, Kristallstrukturen und Raman-Spektren. *Zeitschrift für Naturforschung*, 58, 620–626.
- Fischer, R. and Pertlik, F. (1975) Verfeinerung der Kristallstruktur des Schafarzikits $FeSb_2O_4$. *Tschermaks Mineralogische und Petrographische Mitteilungen*, 22, 236–241.
- Frost, R.L. and Bahfenne, S. (2010a) Raman spectroscopic study of the antimonate mineral bahianite $Al_5Sb_5^+O_{15}(OH)_2$. *Journal of Raman Spectroscopy*, 41, 207–211.
- (2010b) Raman spectroscopic study of the arsenite minerals leiteite $ZnAs_2O_4$, reinerite $Zn_3(AsO_3)_2$ and cafarsite $Ca_3(Ti,Fe,Mn)_7(AsO_3)_{12} \cdot 4H_2O$. *Journal of Raman Spectroscopy*, 41, 325–328.
- Ghose, S., Sen Gupta, P.K., and Schlemper, E.O. (1987) Leiteite, $ZnAs_2O_4$: A novel type of tetrahedral layer structure with arsenite chains. *American Mineralogist*, 72, 629–632.
- Hirschle, C. and Röhr, C. (2000) Alkalimetall-Oxoantimonate: Synthesen, Kristallstrukturen und Schwingungsspektren von $ASbO_2$ (A = K, Rb), $A_3Sb_3O_9$ (A = K, Rb, Cs) und Cs_3SbO_4 . *Zeitschrift für anorganische und Allgemeine Chemie*, 626, 1305–1312.
- Lee, C. and Harrison, W.T.A. (2004) The *catena*-arsenite chain anion, $[AsO_2]_n^{n-}$: $(H_3NCH_2CH_2NH_3)_{0.5}[AsO_2]$ and $NaAsO_2$ (revisited). *Acta Crystallographica*, C60, m215–m218.
- Mellini, M. and Merlino, S. (1979) Versiliaite and apuanite: Derivative structures related to schafarzikite. *American Mineralogist*, 64, 1235–1242.
- Mellini, M., Merlino, S., and Orlandi, P. (1979) Versiliaite and apuanite, two new minerals from the Apuan Alps, Italy. *American Mineralogist*, 64, 1230–1234.
- Menary, J.W. (1958) The crystal structure of sodium polymetaarsenite $(NaAsO_2)_x$. *Acta Crystallographica*, 11, 742–743.
- Pertlik, F. (1975) Verfeinerung der Kristallstruktur von synthetischem Trippkeite, $CuAs_2O_4$. *Tschermaks Mineralogische und Petrographische Mitteilungen*, 22, 211–217.
- (1977) Zur synthese von kristallen von $CuAs_2O_4$ (trippkeit) und $Cu_2As_3O_6CH_3COO$ (eine komponente des farbpigments Schweinfurter Grün). *Zeitschrift für anorganische und Allgemeine Chemie*, 436, 201–206.
- Sejkora, J., Ozdin, D., Vitalos, J., Tucek, P., Cejka, J., and Duda, R. (2007) Schafarzikite from the type locality Pernek (Malé Karpaty mountains, Slovak Republic) revisited. *European Journal of Mineralogy*, 19, 419–427.
- Sykora, R.E., King, J.E., Illies, A.J., and Albrecht-Schmitt, T.E. (2004) Hydrothermal synthesis, structure, and catalytic properties of $UO_2Sb_2O_4$. *Journal of Solid State Chemistry*, 177, 1717–1722.
- Tossell, J.A. (1997) Theoretical studies on arsenic oxide and hydroxide species in minerals and in aqueous solution. *Geochimica et Cosmochimica Acta*, 61, 1613–1623.
- Zemann, J. (1951a) Formel und Kristallstruktur des Schafarzikits. *Tschermaks Mineralogische und Petrographische*, 2, 166–175.
- (1951b) Formel und Kristallstruktur des Trippkeits. *Tschermaks Mineralogische und Petrographische Mitteilungen*, 2, 417–423.

MANUSCRIPT RECEIVED OCTOBER 5, 2010

MANUSCRIPT ACCEPTED JANUARY 18, 2011

MANUSCRIPT HANDLED BY GRANT HENDERSON